ISSN 1022-8594
JEAC

Jahangirnagar University Journal of Science
Vol. 45, No. 2, pp. 1—20

DRIFTS Studies and Quantification of Water uptake experiments onto Iron(II) fumarate, Polyguaiacol and Polycatechol particles

Mohammad Aminur Rahman*

Department of Chemistry, Jahangirnagar University, Savar, Dhaka 1342, Bangladesh

Abstract

This research investigates the hygroscopic properties of organic and organometallic polymeric particles, namely Iron(II) fumarate, Polyguaiacol and Polycatechol. These particles are efficiently formed in iron-catalyzed reactions with aromatic and aliphatic dicarboxylic acid compounds which were detected in field-collected Secondary Organic Aerosol (SOA). The structure of surface water was studied using diffuse reflectance infrared Fourier transform spectroscopy (DRIFTS). Spectroscopic data show that water bonding with organic functional groups acting as hydrogen bond acceptors causes shifts in their vibrational modes. Analysis of the hydroxyl group stretching region revealed weak and strong hydrogen bonding networks that suggest cluster formation reflecting water-water and water-organics interactions, respectively. A modified Type II multilayer Brunauer-Emmett-Teller (BET) adsorption model described the adsorption isotherm on thematerials,Fe-fumarate, polycatechol and polyguaiacol.Modified BET analysis shows that multilayer adsorption takes place for model organic compounds.

Keywords: Aerosol, DRIFTS, Organic matter, Relative Humidity, Carboxylic acid, HULIS.

1. Introduction

Atmospheric aerosol influences the Earth's climate both directly and indirectly.[1] It does this directly through light absorption and scattering, and indirectly by providing surfaces for reaction and modifying cloud formation and lifetime.They also reduce visibility and cause harmful effect on human health.[2,3] Aerosols have a complex chemical compositionwith organic (such as humic-

*Author for correspondance e-mail: mrahman@juniv.edu

like substances, HULIS) and inorganic matters (such as mineral dust).[4] It is well documented that organic-containing aerosols influence the physical and chemical properties of aerosol and thus have effect on the atmosphere and climate through interaction with reactive trace gases, water vapor, clouds, precipitation, and radiation.[5]Moreover, it can contribute significantly to the change in the radiative balance of the atmosphere through their ability to form cloud condensation nuclei (CCN) and ice nuclei (IN).On the other hand, water is an important component of atmospheric aerosols that interact with organic-containing aerosols in various ways.[6,7] Thus, water uptake behavior of organic-containing aerosols can always alteration the structure and oxidation state of organic functional groups by aerosol aging. HULIS have been found as a significant portion of atmospheric organic aerosols that play important role in aerosol aging.[8]

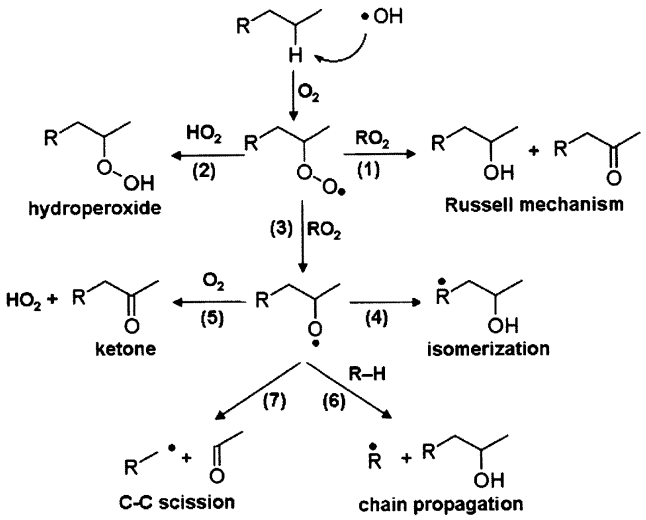

Figure 1. Scheme for the general organic compounds in the atmosphere, in both gas and condensed phases.[9]

Chemical aging of organic aerosols may occur through oxidation of organic compounds in the atmosphere in either the gas phase or the condensed phase as shown by the various mechanisms studied previously Figure 1.[9]

In most cases, oxidation is initiated by a hydrogen abstraction step, in which a hydroxyl radical (·OH) reacts with the organic compound to form an alkyl radical. The subsequent reaction pathways lead either to the addition of functional groups to the carbon backbone of the molecule, which tends to lower the molecule's volatility, or to carbon-carbon bond scission, which frequently increases volatility**.** Additionally, oxidation of unsaturated hydrocarbons may also occur by an ozonolysis pathway, in which an alkene reacts directly with O_3 to form an ozonide intermediate before forming more heavily oxidized products.[10] However, due to the complex nature, aging ofHULISin aerosols is less-studied compared to simple organic compounds with a few functional groups. It has been reported[11] that atmospheric HULIS contain conjugated carbonyl, ethers, aromatic phenols, carboxylic groups, alcohols, oxygenated aliphatic carbons, branched alkyl chains, and a high level of aromatic and aliphatic content. Therefore, most of the studies have used surrogates of atmospheric HULIS that contain aforementioned functional groups, to understand the structural changes of HULIS in the atmosphere.[12] Several studies have been reported in the literature on hygroscopicity and water uptake behavior of organic surrogate compounds of HULIS using various instruments. Most recently,[13] the hygroscopic growth factors for organic surrogate compoundswere observed using a hygroscopicity tandem differential mobility analyzer (HTDMA).The results varied for each compound during dehydration experiments, depending on their chemical composition. It was found that levoglucosan and humic acid aerosol particles release waterupon dehumidification in the range from 90 to 5% relative humidity (RH). However, 4-Hydroxybenzoic acid aerosolparticles remain in the solid state upon dehumidification and exhibit a small shrinking in size at higher RH compared to the dry size. Moreover,they studied the effect of organic components on the hygroscopicity behavior of mixtures containing ammonium sulfate(AS) in relation to the different mass fractions of organiccompounds.[13] Shi *et al.*[14] investigated the hygroscopicity of internally mixed $(NH_4)_2SO_4$(AS)/citric acid (CA) particles by a

pulsed RH controlling system and a rapid scan vacuum FTIR spectrometer(PRHCS-RSVFTIR). It was observed that the half-life time ratio between the water content in the CA particles and the gas phase under RH pulsed change was greater than one under low RH conditions (<40% RH), indicating the significant water transfer limitation due to the high viscosity of CA aerosols at low RH, especially at RH<20%. In addition, water diffusion constants between 10^{-12} m^2 s^{-1} and 10^{-13} m^2s^{-1} in micron size CA aerosols were obtained in a sub-second and second timescale. The addition of AS enhanced the water transfer limitation in the mixed aerosols. The efflorescence relative humidity (ERH) of the mixed particles with AS/CA by molar ratio 3:1 was found between 22.7% and 5.9%. No efflorescence process was observed for the 1:1 mixed particle, indicating that CA greatly suppressed nucleation of AS. The results show that the PRHCS-RSVFTIR is an effective way to simulate hygroscopicity and water transport of aerosols under fast variations in RH in atmosphere.[14]

Cooking organic aerosol (COA) contributesa significant fraction of organic particulate matter in urban areas. Recently, Y. Li *et al.*[15] carried out organic aerosol (COA) chemical aging experiments using aerosol produced by grilling hamburgers, in a smog chamber in the presence of UV light or excess ozone. They measured the water solubility distributions, cloud condensation nuclei (CCN) activity, and corresponding hygroscopicity of fresh and aged COA. The results show that, the average mobilityequivalent activation diameter of the fresh particles at 0.4% supersaturation ranged from 87 to 126 nm anddecreased for aged particles, ranging from 65 to 88 nm. Most of the fresh COA had water solubility less than0.1 g L^{-1}, even though the corresponding particles were quite CCN active. After aging it was found that the COA fraction withwater solubility greater than 0.1 g L^{-1} increased more than 2 times.[15]In another study, George *et al.*[16]employed a Fourier transform infrared (FT-IR) spectroscopic technique to identify and quantify the functional group that originate from phenolic secondary organic aerosol (SOA). Solutions containing an oxidant

(hydroxyl radicalor 3,4-dimethoxybenzaldehyde) and either one phenol (phenol, guaiacol, or syringol) or a mixture of phenols were irradiated to make SOA, atomized, andcollected on a filter. The carbonyl functional group accounts for 3-12% of the SOA sample mass insingle phenolic SOA samples and 9-14% of the SOA sample mass in mixture samples. Comparing carbonyls measured by FT-IR (which could include aldehydes, ketones,esters, and carboxylic acids) with eight small carboxylic acids measured by ion chromatography showsthat the acids only account for an average of 20% of the total carbonyl reported by FT-IR.[16] Cowen *et. al.*[17]selected tannic acid (TA)(Figure 2.) a surrogate of HULIS and conducted photochemical studiesusing diffuse reflectanceinfrared spectroscopy (DRIFTS) as a function of time (3 h), relative humidity (5–30%) and totalirradiance (7, 20, 290 W m^{-2} at 555 nm).

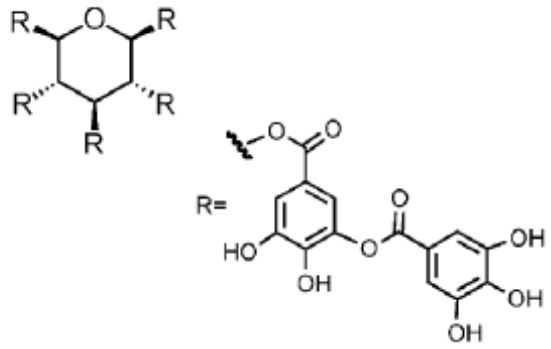

Figure 2. Structure of tannic acid (TA).

*In situ*e xperiments were performed to investigate the photodegradation of solid tannic acid; structure of adsorbed water before and after photodegradation and finally, the change in the hydrophilic behavior of tannic acid due to thisphotochemistry.[17]From the spectral analysis it was found that the structure of water adsorbed on TA comparable with water at the interface with polar organic solvents. Moreover, difference spectral data analysis showed loss features in the 1700–1000 cm^{-1} range and growth in carbonyl features that are blue shifted relative to the starting material, revealed that oxidative photodegradation of TA and formation of aryl aldehydes.[17]

Motivated by the above-mentioned studies and the limited number of experimental works on the heterogeneous chemistry of atmospheric HULIS, we report herein in situ and surface sensitive spectroscopic studies on organic surrogates such as iron (II) fumarate, polycatechol and polyguaiacolas a function of relative humidity under atmospheric pressure and temperature. The main purposes of these studies are as follows to explore in situ and surface sensitive spectroscopic study of water adsorption on model HULIS compounds like iron (II) fumarate, Polycatechol and Polyguacol(Figure 3.) as a function of time and relative humidity. To compare the water uptake behavior of three selected model compounds. To quantify the water adsorption on the model compounds by generating adsorption isotherm.

A) **B)**

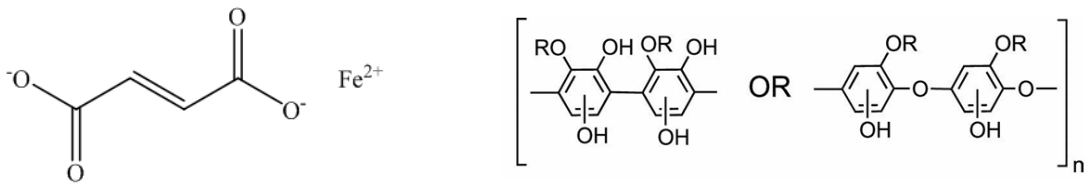

R = H or CH_3

Figure 3. Structure of Iron(II) fumarate (A), (B) polycatechol(R=H) and polyguaiacol (R= CH_3).

2. Experimental

Chemicals All the chemicals were used as received without further purification: catechol (1, 2-benzendiol, >99%, Sigma-Aldrich), guaiacol (2-methoxyphenol, ≥98%, Sigma-Aldrich), fumaric acid (FA, trans-butenedioic acid, ≥99%, Sigma-Aldrich) and iron(III) chloride hexahydrate ($FeCl_3 \cdot 6H_2O$, Sigma-Aldrich). Aqueous phase solutions were prepared by dissolving the chemicals in Milli-Q water (8.5 MΩ cm) with an ionic strength adjusted to 0.01M by adding potassium chloride (KCl powder, 99.0-100.5%, Sigma-Aldrich) to stabilize the pH reading. The

pH was adjusted using solutionsof hydrochloric acid (HCl 6 N, EMD) and sodium hydroxide (NaOH pellets, BDH).

Preparation of Iron(II) fumarate,polycatechol and polyguaiacol

Iron(II) fumarate, Polycatechol and polyguaiacol were synthesize according to published procedure.[1] At first, the organic solutions (Fumaric acid/catechol/guaiacol)(0.001 M) were prepared by dissolving the organics in Milli-Q water (100 mL) of 0.01 M KCl solution. The pH was adjusted to 3 using solutions of concentrated HCl and NaOH solutions. Then, 2 mL of concentrated (0.1 M) solution of $FeCl_3.6H_2O$ was prepared to avoid dilution and achieve the final molar ratio 1:2 (organics/Fe) and added to the organics solutions. The final concentration of $FeCl_3.H_2O$ was 0.0019 M in the solution mixture. The solutions of organics and iron were stirred in the dark (the beaker was wrapped with aluminum foil) for 2 hr and then filtered on nylon membrane filters (0.2 μm pore size, 25 mm dia., EMD). After filtration, the products were air dried overnight. The filters were weighed before and after filtration to measure the mass of the product.

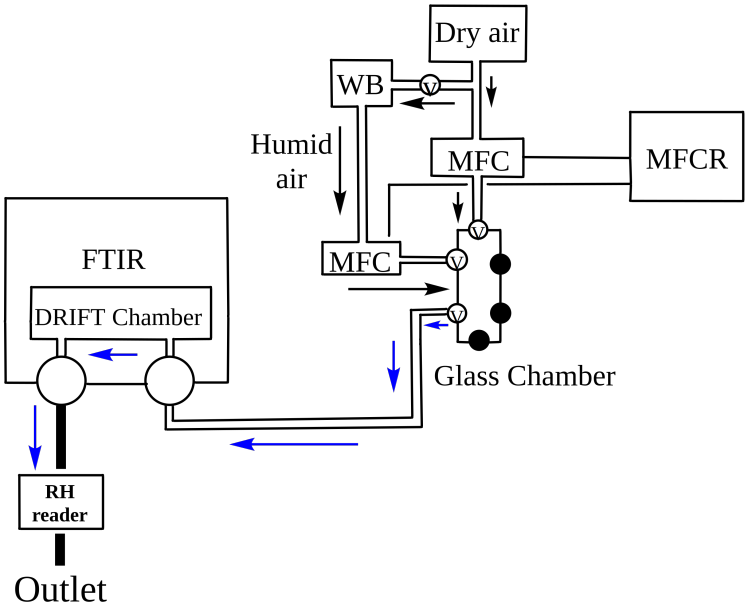

Figure 4. Schematic representation of the DRIFT apparatus and gas handling system. TC is thermocouple, RH refers to relative humidity, V refers to valves, MFC is mass flow controller, MFCR means readout for the mass flow controllers and WB is the water bubbler.

Sample preparation

DRIFTS spectra were collected using a Praying Mantis diffuse reflectance accessory (Harrick, DRK-4-NI8) with a high temperature stainless steel reaction chamber treated with a special SilcoSteel-CR coating. The reaction chamber contains a sample cup (depth 3 mm, dia. 6 mm) and was covered with a treated stainless-steel cover equipped with two ZnSe optical windows and a central quartz viewing window. The DRIFTS accessory was installed in a Nicolet 8700 FTIR spectrometer (Thermo Instruments) equipped with a purge gas generator and a liquid N_2-cooled MCT detector. All spectra were collected at 8 cm^{-1} resolution by averaging 100 scans/spectrum. The temperature of the reaction chamber was monitored by thermocouples connected to a temperature controller (Harrick ATC-024-1). The chamber has two ports for flow mode experiments and was connected to the gas handling system as shown in Figure4, which was

constructed from PFA tubing and fittings (Swagelok). Purged air (Parker Balston Analytical Gas Systems FT-IR Purge Gas Generator 75–52) is separated into two streams: one enters a water bubbler (Dimaglass) containing 18.2 MO water (Millipore Milli-Q Plus) to generate humid air, and the second stream remains dry. Using mass flow controllers (MKS Type 1479A MFC) and a readout (MKS Type 247D), the flow rates of the humid and dry air were altered to vary the relative humidity (RH) of mixed air entering the sample chamber. A relative humidity sensor (Vaisala HUMICAP HM70) was used to monitor the relative humidity of air exiting the chamber.For DRIFTS measurements to be reproducible, the sample must be as homogeneous and well-packed as possible. Since the model organic compounds display high absorbance in the IR region, the sample was diluted with a relatively efficient scattering material that is non-hygroscopic and unreactive. Diamond powder (used as is, Lands Superabrasives LST600T, particle size 5±2 μm, BET area 0.89 ± 0.02 m^2 g^{-1}) was found to fulfil these conditions. Organics was mixed with diamond powder in ratios of 1–6% wt/wt, respectively, and shaken for 1 min using the wig-L-bug withusing the grinding ball. About 0.23 g of the mixture filled the sample cup in the reaction chamber, and a 4 kg press was used for 10 min for reproducible packing. Single beam spectra were collected for diamond powder as a reference and mixed Organics/diamond samples as a function of concentration.

3. Results and Discussion

Infrared characterization of model Organic compounds

Iron (II)fumarate, polycatechol and polyguaiacol were chosen as model compounds as mentioned earlier. Figure5 shows the DRIFTS absorbance spectra 1-6% (wt/wt) of (a) Iron (II) fumarate (b) polycatechol and (c) polyguaiacolin diamond and assignment of the observed bands and corresponding functional groups have been summarized in Table 1.

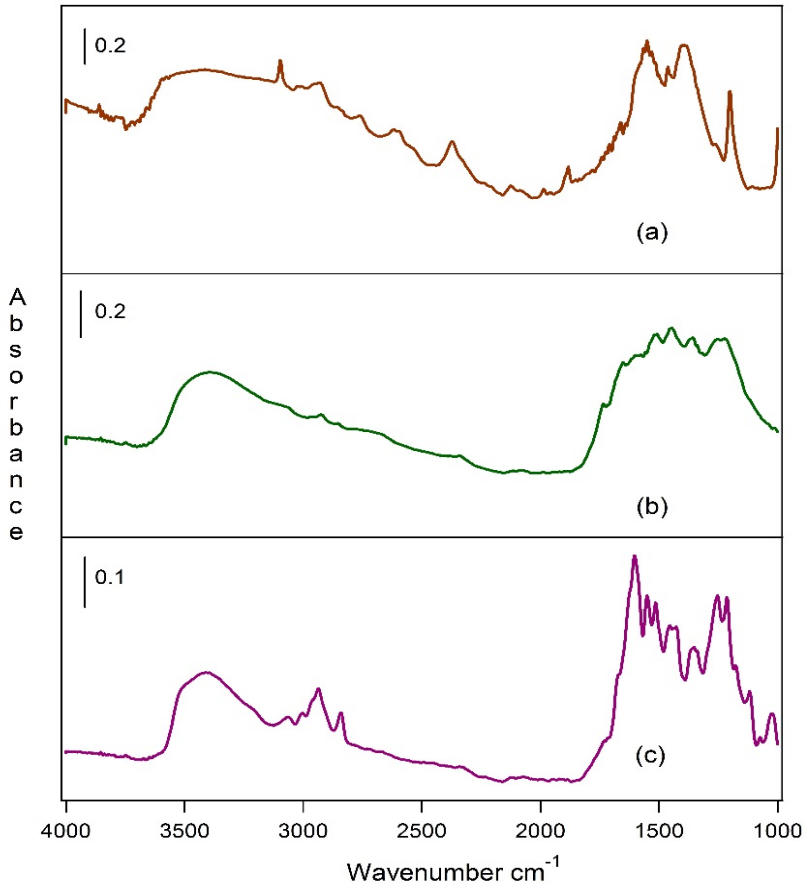

Figure 5. DRIFTS absorbance Spectra of (a) Iron (II) fumarate (b) Polycatechol and Polyguaiacol in diamond 1-6% (wt/wt) (%RH< 1%).

The assignment is based on the chemical structure of three organic compounds Iron (II) fumarate, polycatechol and polyguaiacol. and was compared with the IR bands observed for atmospheric HULIS.[17] The spectral range1800–1000 cm^{-1} contains bands assigned to the stretching vibration of C-O at 1080 and 1209 cm^{-1}; Aromatic ring breathing vibration and C-H in-plane deformation at 1319 cm^{-1}; Stretching vibration of aromatic C-C bonds at 1450, 1545 and 1616 cm^{-1} and stretching vibration of unconjugated C=O group in ester links [-C(O)O-] between polyphenol substituents at 1713 cm^{-1}.

Table 1. Assignment of bands and corresponding functional groups for the model organic compounds

Functional groups	**Wavenumber cm^{-1}**
C-O	1080, 1209
C-H	1319
C-C	1450, 1525, 1616
C=O	1700
-C(O)O-	1713
-OH	3392
C-H	3000-2850
$-CH_2$	3000-2850
$-CH_3$	3000-2850

The stretchingvibration of OH phenolic groups exhibits a broad featurecentered at 3392 cm^{-1}. Moreover, the IR spectra of the organics shows bands in the spectral range 3000–2850 cm^{-1} which are assigned to the C–H stretching vibration of methyl ($–CH_3$) and methylene ($–CH_2–$) groups of aliphatic chains.[17]

Water adsorption on model Organic compounds

The spectra of water adsorbed on the surface of iron(II) fumarate particle as function of relative humidity (RH) between 0.02 to 85 %, are shown in Figure 5. Single beam spectra were collected as a function of RH and referenced to the spectrum of dry iron(II) fumarate/diamond, followed by subtracting absorptions due to gas phase water. These difference absorbance spectra show that increasing RH results in increasing the intensity of spectral features assignedto adsorbed water, which are the bending mode $\delta(H_2O)$ at1640 cm^{-1} and the stretching vibration of hydrogen

bonded OH groups ν(OH) between 3650 and 3000 cm^{-1}. The bending mode was used to quantify the relative amounts of adsorbed water on the surface of iron (II) fumarate (vide infra).

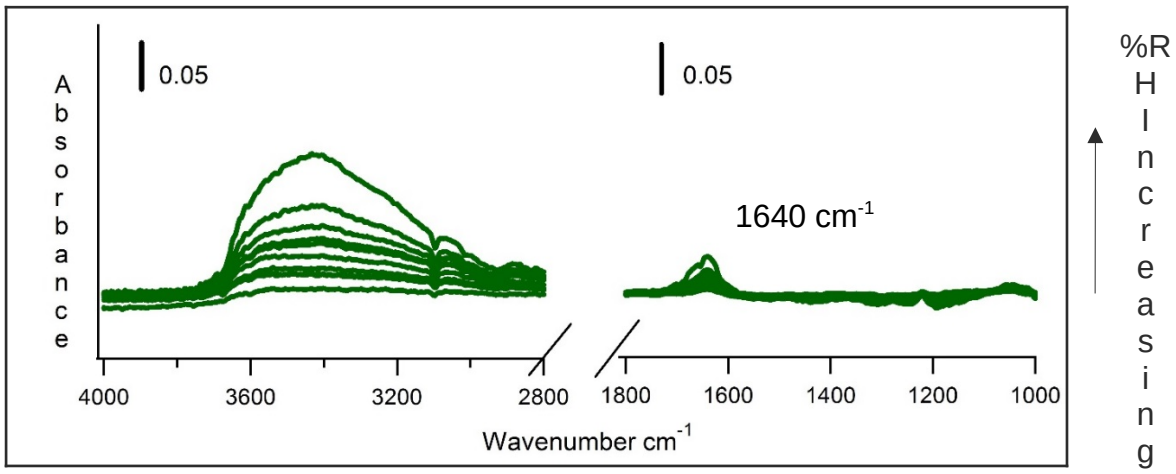

Figure 6. DRIFT absorbance spectra of water uptake on Iron (II) Fumarate with increasing RH.

Figure 7 shows the absorbance spectra water adsorption on polycatechol particle as a function of increasing RH from 0.02 to 85.0 %.Single beam spectra were collected as a function of RH and referenced to the spectrum of dry polycatechol/diamond, followed by subtracting absorptions due to gas phase water. These difference absorbance spectra show that increasing RH results in increasing the intensity of spectral features assigned to adsorbed water, which are the bending mode $\delta(H_2O)$ at1635 cm^{-1} and the stretching vibration of hydrogen bonded-OH groups ν(OH) between 3650 and 3000 cm^{-1}. The bending mode was used to quantify the relative amounts of adsorbed water on the surface of polycatechol(vide infra)

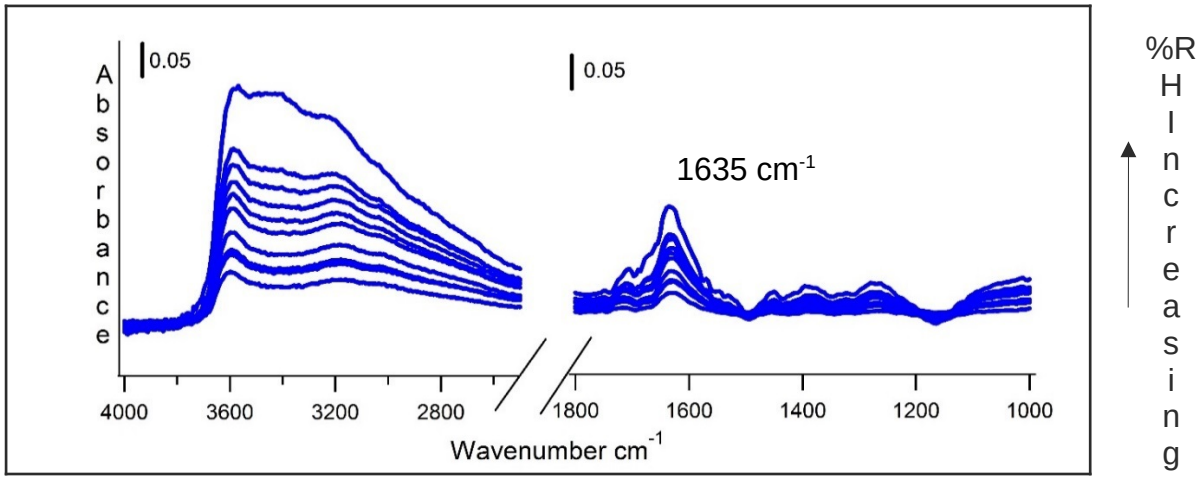

Figure 7. DRIFT absorbance spectra of water uptake on polycatechol with increasing RH.

Figure8 shows the absorbance spectra water adsorption on polyguaiacol particle as a function of increasing RH from 0.02 to 85.0 %.

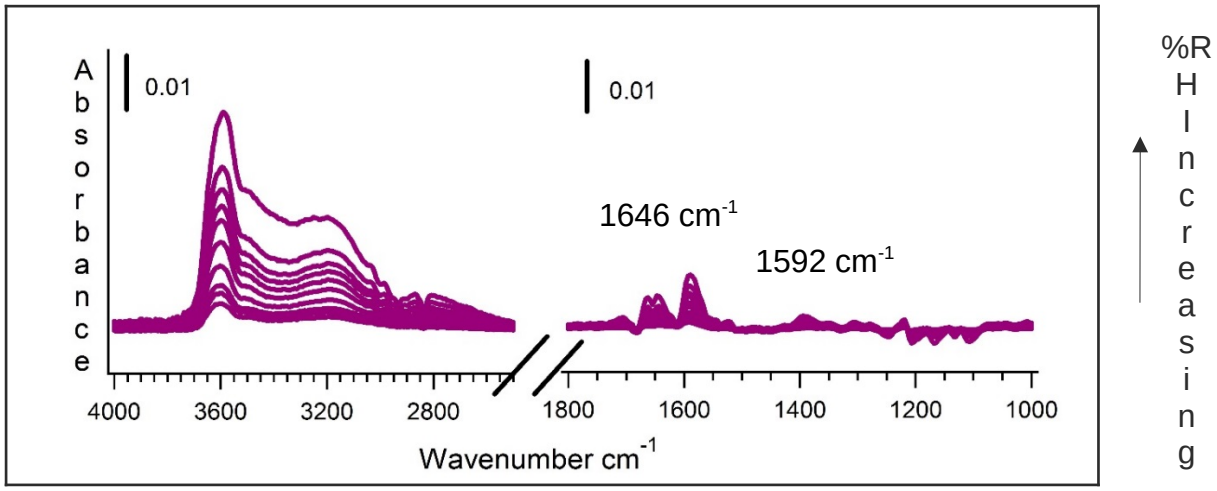

Figure 8. DRIFT absorbance spectra of water uptake on polyguaiacol with increasing RH.

Single beam spectra were collected as a function of RH and referenced to the spectrum of dry polyguaiacol/diamond, followed by subtracting absorptions due to gas phase water. These difference absorbance spectra show that increasing RH results in increasing the intensity of spectral features assigned to adsorbed water, which are the bending mode $\delta(H_2O)$ at1646 cm^{-1} and the stretching vibration of hydrogen bonded -OH groups ν(OH) between 3650 and 3000 cm^{-1}.

However, water adsorption on polyguaiacol shows an addition band at 1592 cm^{-1}. To confirm the peak is not due to solvent, we run controlled experiment in D_2O. Figure 9 shows the absorbance spectra of D_2O adsorption on polyguaiacol particle as a function of increasing RH from 0.02 to 85.0 %. The bending mode at 1646 $cm^{-1}$was used to quantify the relative amounts of adsorbed water on the surface of polycatechol(vide infra).

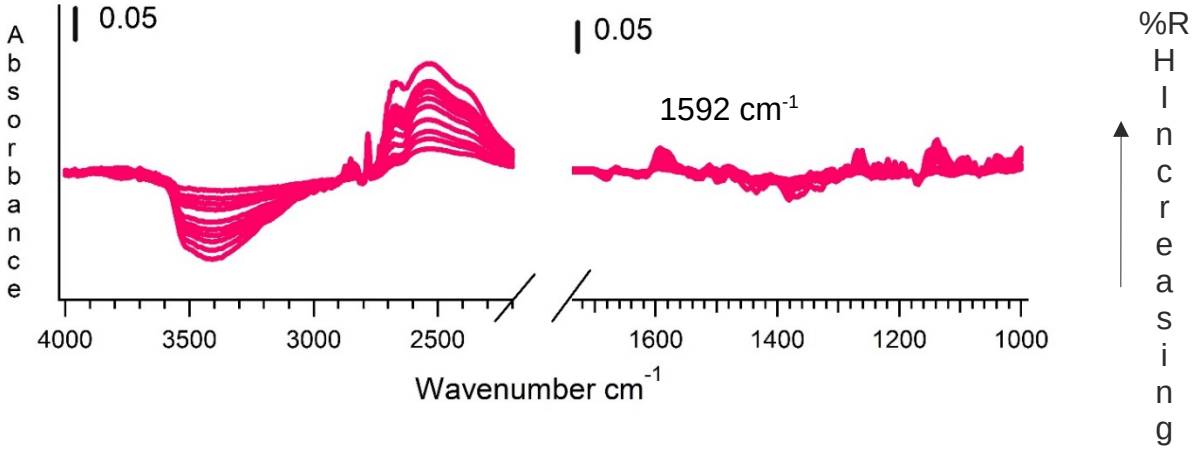

Figure 9. DRIFT absorbance spectra of D_2O uptake on polyguaiacol with increasing RH.

Quantification ofWater uptake experiment by generating adsorption isotherm curves

The coverage of adsorbed water on iron (II) fumarate, polycatechol and polyguaiacolcan be quantified by generating adsorption isotherm curves. The bending mode absorption band of surface adsorbed water is integrated, and integrated absorbance is converted to the number of adsorbed water layers and plotted against relative humidity, P/P_0. The number of adsorbed water layers is assumed to be a linear function of the integrated absorbance of the bending mode. If the data represented exhibit the shape of a type II ors-shaped adsorption isotherm curve, indicates multilayeradsorption is occurring. Therefore, BET model was chosen for the analysis.[18] However, if adsorption takes place on a uniform surface and an infinite number of layers ($n = \infty$) build up on

the surface at the saturation vapor pressure of the adsorbing gas, then most type II adsorption isotherms can be fit to the two-parameter BET eq. 1.

$$V = \frac{V_m c \frac{P}{P_0}}{\left(1 - \frac{P}{P_0}\right)\left(1 - \frac{P}{P_0} + c\frac{P}{P_0}\right)} \qquad \text{... 1}$$

where V is the volume of gas adsorbed at equilibrium pressure P, V_m is volume of gas necessary to cover the surface of the adsorbent with a complete monolayer, P is the equilibrium pressure of the adsorbing gas, and $P0$ is saturation vapor pressure of the adsorbing gas at that temperature. The parameter c is the temperature-dependent constant related to the enthalpies of adsorption of the first and higher layers through eq. 2.

$$c = \exp -\left[\frac{\Delta H_1^\circ - \Delta H_2^\circ}{RT}\right] \qquad \text{...2}$$

where $\Delta H°_1$ is the standard enthalpy of adsorption of the first layer, $\Delta H°_2$ is the standard enthalpy of adsorption on subsequent layers and is taken as the standard enthalpy of condensation, R is the gas constant, and T is the temperature in Kelvin.

Mostly,[18]the two-parameter BET equation shown above does not fit the experimental data at the highest pressures when the adsorption isotherm rises indefinitely and an infinite number of layers ($n = \infty$) of adsorbing gas is predicted to build up onthe surface. A three-parameter BET eq. 3 limits the number of layers of gas adsorbing at high values of $P/P0$. The three parameter BET equation is then takes the form as below

$$V = \left[\frac{V_m c\left(\frac{P}{P_0}\right)}{1 - \left(\frac{P}{P_0}\right)}\right]\left[\frac{1 - (n+1)\left(\frac{P}{P_0}\right)^n + n\left(\frac{P}{P_0}\right)^{n+1}}{1 + (c-1)\left(\frac{P}{P_0}\right) - c\left(\frac{P}{P_0}\right)^{n+1}}\right] \qquad \text{... 3}$$

where P, P_0, V, V_m, and c are defined as eq. 1 and2 and n is an adjustable parameter given as the maximum number of layers of the adsorbing gas and is related to the pore size and properties of the adsorbent. As a result, multilayer formation of adsorbing gas is limited to n layers at large valuesof $P/P0$. Equation 3 models experimental data well when a finite number of layers are observed for adsorption of gases on a porous surface. The three-parameter BET equation was used to obtain a fitto the experimental data. The parameters n, V_m, and c can be calculated according to the method discussed in detail by Joyneret al., in which eq 3 is rearranged into the linear form, shown in eq 4

$$\frac{\Phi(n,x)}{V} = \frac{1}{V_m C} + \frac{\theta(n,x)}{V_m} \qquad \text{... 4}$$

where

$$\Phi(n,x) = \frac{X[(1 - X^n) - nX^n(1 - X)]}{(1 - X)^2}$$

$$\theta(n,x) = \frac{X(1 - X^n)}{1 - X}$$

and

$$X = P/P_0$$

Thus, we quantify our data for the model organics iron (II) fumarate, polycatechol and polyguaicol with modified BET analysis as shown in Figure10. The results are summarized in Table 2. Modified BET analysis shows that multilayer adsorption take place for model organic compounds. The standard enthalpies of the first layer ΔH_1 values for polycatecholis larger than that of iron (II) fumarate and polygamical.

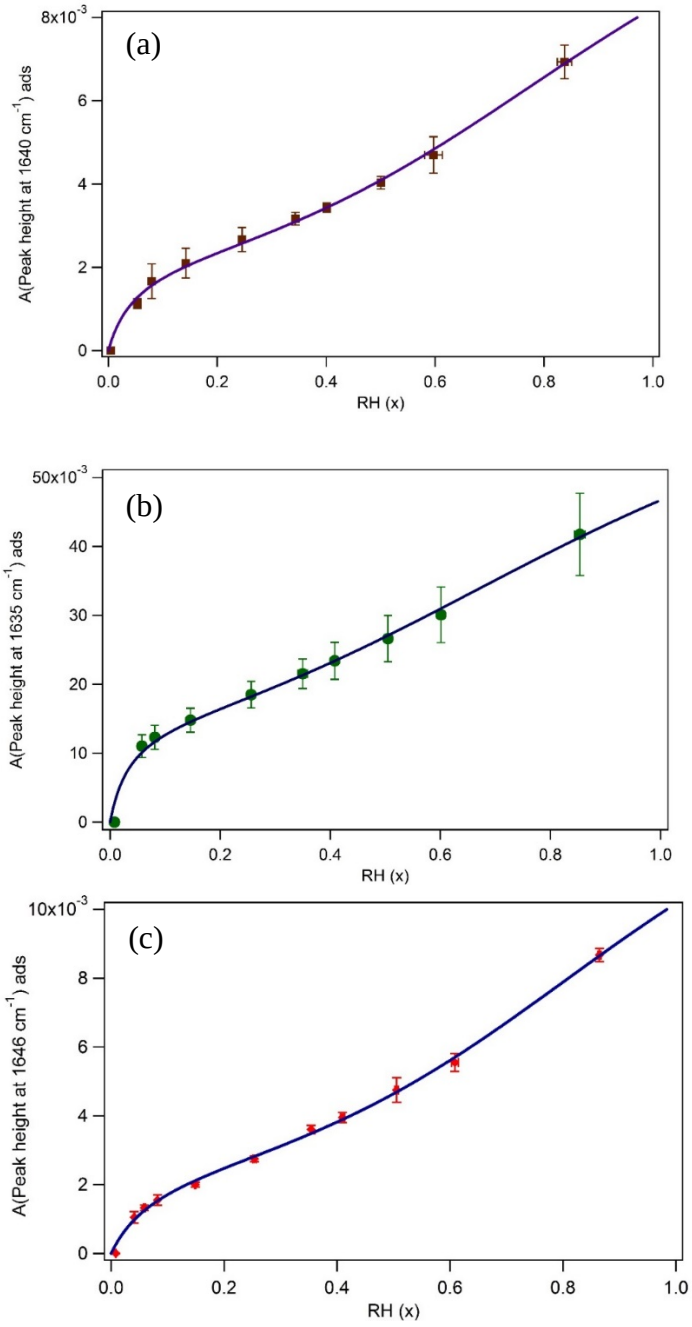

Figure 10. Water uptake on organics (a) iron (II) fumarate,(b) polycatechol and (c) polyguaiacolas a functionof increasing relative humidity. The integrated area of the water-bending mode for each organic was determined as a function of relative humidity. The filled solids represent experimental data for water uptake on organic particles. The solid lines represent the BET fit of the experimental data according to eq 3.

Table 2. Adsorption Parameters for Water Uptake on Iron (II) fumarate, polycatechol and polyguaiacol particles

Sample	n	c	ΔH_1(KJ/moL)	Range of relative humidity
Iron (II) fumarate	6	21.01±7	-51.54±0.66	0.0075-0.081
Polytcatechol	5	28.38±16	-52.28±0.26	0.0079-0.085
Polyguaiacol	7	22.03±9	-51.66±1.31	0.0076-0.086

Conclusion

Water uptake experiments of three model compounds Iron(II) fumarate, Polycatechol and Polyguaiacol were performed by DRIFT spectroscopic analysis. Water adsorption took place for all the model compounds and formed multilayer as evident from spectral data analysis. We were able to quantify the parameters from the adsorption of H_2O on the surface on particles using modified BET analysis. Here, the standard enthalpies of the first layer ΔH_1 values for polycatechol is larger than that of iron (II) fumarate and polyguaiacol. Results from these studies are significant due to it's relevance to the role of water in various chemical transformations in the atmosphere. The thermodynamic parameters obtained from these experiments may show a pathway for future research.

References

[1] Slikboer, S.; Grandy, L.; Blair, S. L.; Nizkorodov, S. A., Smith, R. W. and Al-Abadleh, H. A. *Environ. Sci. Technol.* 2015, **49**, 7793.

[2] Watts, N.; Adger, W. N.; Agnolucci, P. *et al.*, *The Lancet-Elsevier*2015, 60854.

[3] Madl, A. K.; Plummer, L. E.; Carosino, C. and Pinkerton, K. E. *Annual review of Physiology*, 2014, **76**, 447.

[4] Prather, K. A.; Hatch, C. D. and Grassian, V. H. *Annu. Rev. Anal. Chem.*2008, **1**, 485.

[5] Fofie, E. A.; Donahue, N. M. and Asa-Awuku, A. *Aero. Sci. Tech.*2018, **52**, 242.

[6] Gu. W.; Li. Y.; Zhu, J.; Jia, X.; Lin, Q.; Zhang, G.; Ding, X.; Song, W.; Bi, X.; Wang, X. and Tang, M. *Atmos. Meas. Tech.*,2017, **10**, 3821.

[7] Burkholder *et. al. Environ. Sci. Technol.* 2017, **51**, 2519.

[8] Graber, E. R. and Rudich, Y. *Atmos. Chem. Phys.* 2006, **6**, 729.

[9] Kroll, J. H.; Smith, J. D.; Che, D. L.; Kessler, S. H.; Worsnop, D. R. and Wilson. K. R. *Phys. Chem. Chem. Phys*,2009, 11, 8005.

[10] Smith, J. D.; Kroll, J. H.; Cappa, C. D.; Che, D. L.: Liu, C. L.; Ahmed, M.; Leone, S. R.; Worsnop, D. R. and Wilson. K. R. *Atmos. Chem. Phys*,2009, **9**, 3209.

[11] Hatch, C. D.; Gierlus, K. M.; Schuttlefield, J. D. and Grassian, V. H, *Atmospheric Environment*, 2008, **42**, 5672.

[12] Lei, T.; Zuend, A.; Cheng, Y.; Su, H.; Wang, W. and Ge, M. *Atmos. Chem. Phys.*2018, **18**, 1045.

[13] Shi, X. M.; Wu, F. M.; Jing, B.; Wang, N.; Xu, L.; Pang, S. and Yun-Hong Zhang, Y. *Chemosphere*,2017, **188**, 532.

[14] Lia, Y.;Tasogloub, A.; Liangouc, A.;Cainb, K. P.;Jahnb, L.;Gub, P.;Kostenidouc, E. and Pandisb, S. N.*Atmospheric Environment*, 2018, **176**, 103.

[15] George, K. M.; Ruthenburg, T. C.; Smith, J.; Yu, L.; Zhang, Q.; Anastasio, C. and Dillner, A. M. *Atmospheric Environment*, 2015, **100**, 230.

[16] Cowen, S. and Al-Abadleh, H. A. *Phys. Chem. Chem. Phys.*,2009, **11**, 7838.

[17] Goodman, A. L.; Bernard, E. T. and Grassian, V. H.*J. Phys. Chem. A*2001,**105**, 6443.

This page is intentionally left Blank